IJC
International Journal of Cancer

A mutant KRAS-induced factor REG4 promotes cancer stem cell properties *via* Wnt/β-catenin signaling

Jeong-Ha Hwang[1,2,3], Junyong Yoon[1,2], Yong-Hee Cho[1,2], Pu-Hyeon Cha[1,2], Jong-Chan Park[1,2] and Kang-Yell Choi[1,2,4]

[1]Translational Research Center for Protein Function Control, Yonsei University, Seoul, South Korea
[2]Department of Biotechnology, College of Life Science and Biotechnology, Yonsei University, Seoul, South Korea
[3]Department of Biomaterials Science and Engineering, Yonsei University, Seoul, South Korea
[4]CK Biotechnology Inc., Seoul, South Korea

Mutant *KRAS* provides a driving force for enhancement of cancer stem cells (CSCs) characteristics contributing transformation of colorectal cancer (CRC) cells harboring *adenomatous polyposis coli* (*APC*) mutations. Here, we identified the factors mediating the promotion of CSCs properties induced by *KRAS* mutation through microarray analyses of genes specifically induced in CRC spheroids harboring both *KRAS* and *APC* mutations. Among them, REG4 was identified as a key factor since CRISPR/Cas9-mediated knockout of REG4 most significantly affected the stem cell characteristics in which CSCs markers were effectively suppressed. We show that REG4 mediates promotion of CSCs properties *via* Wnt/β-catenin signaling in various *in vitro* studies including tumor organoid systems. Furthermore, expression patterns of CSCs markers and REG4 correlated in intestinal tumors from $Apc^{min/+}/Kras^{G12D}LA2$ mice and in CRC patient tissues harboring both *KRAS* and *APC* mutations. The role of REG4 in the tumor-initiating capacity accompanied by enhancement of CSCs characteristics was also revealed by NSG mice xenograft system. Collectively, our study highlights the importance of REG4 in promoting CSCs properties induced by *KRAS* mutation, and provides a new therapeutic strategy for CRC harboring both *APC* and *KRAS* mutations.

Introduction

Colorectal cancer (CRC) results from the cumulative effects of multiple and sequential genetic alterations, including mutations of *adenomatous polyposis coli* (*APC*) tumor suppressor gene and *KRAS* proto-oncogene, leading to the activation of the Wnt/β-catenin and Ras/extracellular-signal-regulated kinase (ERK) pathways, respectively.[1,2] Inactivating mutations in the *APC* gene, found in as high as 90% of CRC patients, promote the initiation of CRC.[3] Activating mutations in the *KRAS* gene, which have been detected in approximately 40% of CRC patients, mostly occur during early and intermediate stages of CRC tumorigenesis.[4,5]

The Ras/ERK pathway interacts with the Wnt/β-catenin pathway during CRC tumorigenesis.[6–8] The *Kras* mutation alone does not induce significant transformation of the intestinal epithelium in mice; however, mutations in both *Apc* and *Kras* synergistically enhanced the transformation effects as demonstrated by the critical increment in both number and growth rate of tumors.[6,7,9] In addition, the interaction of Wnt/β-catenin and RAS/ERK pathways plays a critical role in malignant phenotypes, and the increase in both β-catenin and RAS levels positively correlate in human CRC harboring *APC* mutations.[10,11] It is known that the tumor malignancies are caused by induction of cancer stem cells (CSCs) originating from a small subpopulation of tumor cells.[12,13] The CSCs-induced effects such as the progression to metastasis and recurrence after initial chemotherapy are the major causes of lethality in patients.[14] However, the mechanism of action and factors mediating the promotion of CSCs properties are poorly understood.

Kras mutation alone does not significantly induce CSCs as previously shown that expression of a mutant *Kras* allele alone in mouse colonic cells failed to expand the stem cell population[15]; however, additional *Apc* mutation results in the induction of CSCs leading to tumor growth as well as liver metastasis.[16]

Additional Supporting Information may be found in the online version of this article.

Key words: *KRAS* mutation, *APC* mutation, REG4, cancer stem cells, colorectal cancer, Wnt/β-catenin signaling

Abbreviations: AD: adherent; APC: adenomatous polyposis coli; CRC: colorectal cancer; CSCs: cancer stem cells; D-MT: DLD-KRAS-MT; D-WT: DLD-KRAS-WT; ERK: extracellular-signal-regulated kinase; FDR: false discovery rate; GSEA: Gene Set Enrichment Analysis; LDA: limiting dilution analysis; LPE: local-pooled-error; NES: normalized enrichment score; NSG: NOD/SCID-IL2Rγ$^{-/-}$; qRT-PCR: quantitative real-time PCR; rhREG4: recombinant human REG4 protein; rmREG4: recombinant mouse REG4; SP: spheroids; TMA: tissue microarray

Conflict of interest: The authors declare no conflict of interest.

Grant sponsor: National Research Foundation of Korea (NRF); **Grant numbers:** 2015R1A2A05001873, 2016R1A5A1004694, 2019R1A2C3002751; **Grant sponsor:** Graduate School of YONSEI University; **Grant sponsor:** Brain Korea 21 (BK21) Plus
DOI: 10.1002/ijc.32728
History: Received 17 Jun 2019; Accepted 1 Oct 2019; Online 12 Oct 2019

Correspondence to: Dr Kang-Yell Choi, E-mail: kychoi@yonsei.ac.kr

What's new?

Mutant *KRAS* is a driving force in the enhancement of cancer stem cell (CSC) characteristics that contribute to the malignant transformation of colorectal cancer (CRC) cells harboring *APC* mutations. However, the factors involved in mutant *KRAS*-mediated induction of CSCs and the underlying mechanisms remain unclear. Here, using organoids, xenograft systems, and colorectal cancer (CRC) patient tissues, the authors show that REG4 is a key factor mediating the promotion of CSC properties induced by *KRAS* mutation and acts *via* the Wnt/β-catenin pathway. These findings provide a new potential therapeutic target for the treatment of CRC harboring both *APC* and *KRAS* mutations.

The induction of CSCs by both *APC* and *KRAS* mutations is attributed to the accumulation of mutant KRAS by *APC* loss owing to the absence of its phosphorylation and subsequent polyubiquitination-dependent proteasomal degradation by the GSK3β inactivation.[16,17] Indeed, the increased mutant KRAS plays a role in the further strong activation of the Wnt/β-catenin signaling *via* a positive feedback loop through the MEK–ERK pathway in addition to its initial activation by *APC* loss.[10,16] However, the mechanism and factors involved in mutant-*KRAS*-mediated induction of CSCs are unknown.

In our study, the factors mediating promotion of CSCs properties induced by *KRAS* mutation were systematically investigated through a microarray analysis of the *APC*-mutated isogenic DLD-1 CRC cells harboring wild-type *KRAS* (D-WT) or mutant *KRAS* (D-MT). We were especially interested in the factors specifically induced in the spheroids (SP) harboring both *APC* and *KRAS* mutations. Among these, REG4 was selected as a factor for further studies since CRISPR/Cas9-mediated knockout of REG4 resulted in the most severe reduction in the stem cell characteristics of CRC cells harboring *APC* and *KRAS* mutations.

REG4 has been known to be involved in cell growth, resistance to apoptosis, and metastasis of various tumors.[18–21] Several reports show that REG4 promotes cell proliferation by inducing Akt-GSK3β-β-Catenin-TCF-4 Signaling or EGFR signaling in colon cancer cell lines such as HCT116 and HT29.[22,23] However, the effect of REG4 induced by mutant *KRAS* on CRC is not well understood. Moreover, to date, the exact role of REG4 in CRC has been still controversial. Some studies showed conflicting results regarding the relationship between REG4 and clinical features in CRC.[24,25] Meanwhile, the Reg4-expressing deep crypt secretory cells are known to provide niche support for $Lgr5^+$ colonic stem cells in colonic crypts,[26] and these colocalized with the $Lgr5^+$ cells in colon adenomas of $Apc^{min/+}$ mice.[13] However, the involvement of REG4 in promoting CSCs in CRC has not yet been characterized.

In the current study, we found that REG4 is a critical factor enhancing CSCs characteristics, and its induction depends on *KRAS* mutation in CRC patient tissues and in intestinal tumors from $Apc^{min/+}/Kras^{G12D}LA2$ mice. Overall, our study reveals that REG4 is a key factor mediating the enhancement of CSCs properties induced by *KRAS* mutation, and thus a potential therapeutic target for CRC involved in promotion of CSCs.

Materials and Methods

Cell culture, transfection and reagents

Isogenic human DLD-1 CRC cell lines expressing either WT or MT *KRAS* (D-WT and D-MT cells, respectively) were provided by B. Vogelstein (Johns Hopkins Oncology Center, Baltimore, MD). Those cells are derived by homologous recombination from DLD-1 parental cells containing both wild-type *KRAS* and mutant *KRAS* (G13D) alleles. The D-WT or D-MT express either the single wild-type *KRAS* allele (WT/−) or the single $KRAS^{G13D}$ allele (G13D/−), respectively.[27] Caco-2 (RRID:CVCL_0025), DLD-1 (RRID:CVCL_0248), LoVo (RRID:CVCL_0399), SW480 (RRID: CVCL_0546) and HCT-15 (RRID:CVCL_0292) were obtained from the American Type Culture Collection (ATCC) (DLD-1 and HCT 15 are derived from the same patient). The isogenic D-WT and D-MT cells were maintained in McCoy's 5A (Modified) medium (Gibco, New York, NY) containing 10% heat-inactivated fetal bovine serum (Gibco) and 1% penicillin–streptomycin (Gibco). DLD-1, LoVo, SW480 and HCT-15 cells were maintained in RPMI 1640 medium (Gibco) containing 10% FBS and 1% penicillin–streptomycin. Caco-2 cells were grown in DMEM supplemented with 20% FBS and 1% penicillin–streptomycin. All human cell lines have been authenticated using short-tandem repeats (STR) profiling within the last 3 years. All experiments were performed with mycoplasma-free cells. For knockdown experiments, D-MT cells were transfected with pLKO.1-Puro or pLKO.1-shKRAS-Puro (Sigma-Aldrich, St. Louis, MO, TRCN0000033261 CDS). Lipofectamine (Invitrogen, Waltham, MA) was used for plasmid transfection, according to the manufacturer's instructions. The following drugs and recombinant proteins were administered at the indicated concentrations: AS703026 (10 μM), doxycycline (1 μg/ml), recombinant human REG4 protein (rhREG4; 25 ng/ml) and recombinant mouse REG4 protein (rmREG4; 25 ng/ml). rhREG4 and rmREG4 were purchased from Sino Biological (Beijing, China). All other chemicals were purchased from Sigma-Aldrich.

SP formation assay

SP were cultured in DMEM/F12 (1:1) medium (Gibco) containing 1 × B27 supplement (Gibco), EGF (100 ng/ml; PeproTech, Rocky Hill, NJ), bFGF (50 ng/ml; PeproTech), heparin (4 μg/ml; Sigma-Aldrich) and 1% penicillin–streptomycin. Cells were plated at a density of 2×10^5 cells per dish in 90 mm petri dish (SPL) and cultured for 3–7 days. SP number and size were quantified using WCIF ImageJ bundle software v1.37a

(University Health Network Research, Toronto, Canada, http://www.uhnresearch.ca/facilities/wcif/fdownload.html).

CRISPR/Cas9 knockout system

D-MT (*REG4*$^{-/-}$, *IL8*$^{-/-}$, *LTB*$^{-/-}$, *CCL20*$^{-/-}$, *PTGS2*$^{-/-}$, *CC2D2A*$^{-/-}$ or *RAB30*$^{-/-}$) cell lines were generated by using the CRISPR-Cas9 system. The guide RNAs targeting specific genes were designed by using the CRISPR gRNA design tool on the DNA2.0 website (https://www.dna20.com/eCommerce/cas9/input). Oligomers coding gRNA were annealed and cloned into the lentiCRISPRv2 plasmid according to the instructions in the manual.[28] For generation of knockout cells, D-MT cells were infected with lentivirus-containing media with polybrene (8 μg/ml; Sigma-Aldrich) for 6 hr. All cells were selected using puromycin (2 μg/ml; Sigma-Aldrich)-containing medium for 20 days, and remaining cells were used for single-cell colony selection in a 96-well cell culture plate. Each cell colony was cultured, and each knockout cell was verified by DNA sequencing. The gRNA sequences used are listed in the table of Appendix S1.

Microarray analysis

Total RNA was amplified and purified using the Ambion Illumina RNA amplification kit (Ambion) to yield biotinylated cRNA according to the manufacturer's instructions. Briefly, 550 ng of total RNA was reverse-transcribed to complementary DNA (cDNA) using M-MLV reverse transcriptase (Invitrogen). Second-strand cDNA was synthesized, transcribed *in vitro* and labeled with biotin-NTP. After purification, the cRNA was quantified using the ND-1000 Spectrophotometer. Seven hundred and fifty nanograms of labeled cRNA was hybridized in each human HT-12 expression v.4 bead array for 16–18 hr at 58°C, according to the manufacturer's instructions (Illumina). Detection of array signal was carried out using Amersham fluorolink streptavidin-Cy3 (GE Healthcare Bio-Sciences, Chicago, IL) following the bead array manual. Arrays were scanned using an BeadArray Reader Microarray Laser Scanning Confocal Microscope System (Illumina), according to the manufacturer's instructions. The quality of hybridization and overall chip performance were monitored by visual inspection of both internal quality control checks and the raw scanned data. Raw data were extracted using the software provided by the manufacturer (Illumina; GenomeStudio [v2011.1] Gene Expression Module v1.9.0). Array probes were logarithmically transformed and quantile-normalized. Statistical significance of the expression data was determined using the local-pooled-error (LPE) test and fold change in the null hypothesis, and no differences existed among the groups. The false discovery rate (FDR) was controlled by adjusting *p*-value using the Benjamini–Hochberg algorithm. Heatmap analysis was performed using MeV v4.0 software according to its manual.

Mouse xenograft assay

For *in vivo* limiting dilution analysis (LDA), approximately 5-week-old male NOD/SCID-IL2Rγ$^{-/-}$ (NSG) mice were purchased from Joongabio Inc. D-MT cells stably expressing a control shRNA or shRNA targeting *REG4* (shRNA #1) were cultured under SP culture conditions for 5 days and were dissociated into single cells using trypsin/EDTA. About 1×10^5, 1×10^4 and 1×10^3 cells were resuspended in 50 μl of PBS: Matrigel (1:1; Corning) and subcutaneously injected into the dorsal flank of NSG mice (n = 10 mice per group). Tumor volumes of mice were measured every 6–8 days. Tumors were measured using Vernier calipers, and tumor volume was calculated according to the following formula: $\pi/6 \times \text{length} \times \text{width} \times \text{height}$. Tumor growth was monitored 10 weeks after injection. Seventy-four days after injection, the mice were sacrificed and the tumors were excised, weighed, and fixed in 4% PFA or snap-frozen in liquid nitrogen for further analysis. The number of tumors formed out of the number of sites injected was scored to determine the frequency of CSCs, which was calculated using the ELDA software (http://bioinf.wehi.edu.au/software/elda/index.html) provided by the Walter and Eliza Hall Institute.[29] For tumor growth assays, approximately 4- to 6-week-old male athymic BalbC nu/nu mice were purchased from Orientbio Inc (Seongnam-si, South Korea). D-MT cells (5×10^6 cells) stably expressing a control shRNA or shRNA targeting *REG4* (shRNA #1 or 2) in 50 μl of PBS: Matrigel (1:1) were subcutaneously injected into the dorsal flank of nude mice (n = 2 mice per group). Thirty days after injection, the mice were sacrificed, and the tumors were collected for further analyses. All animal experiments were performed in accordance with Korean Food and Drug Administration guidelines. Protocols were reviewed and approved by the Institutional Review Board of Severance Hospital, Yonsei University College of Medicine.

Animal models and tissue preparation

C57BL/6J-*Apc*$^{\text{min}/+}$ (*Apc*$^{\text{min}/+}$), B6.129S-*Kras*^{tm3Tyj} (*Kras*^{G12D}*LA2*), and C57BL/6J-*Axin2*^{lacZ} (*Axin2*^{lacZ}) mice were obtained from Jackson Laboratory. B6.129P2-*Lgr5*$^{tm1(cre/ERT2)Cle}$*/J* (*Lgr5-EGFP*) mice were obtained from Dr. Young-Yun Kong (Seoul National University, Seoul, Korea). To generate *Apc*$^{min/+}$*/Kras*^{G12D}*LA2*, *Apc*$^{min/+}$*/Axin2*^{lacZ} or *Apc*$^{min/+}$*/Lgr5-EGFP* mice, *Apc*$^{min/+}$ mice were crossed with *Kras*^{G12D}*LA2*, *Axin2*^{lacZ} *or Lgr5-EGFP* mice, respectively. Mouse genotyping was performed using genomic DNA extracted from the tail. To account for genetic background effects, sex-matched littermates were always used as controls.

Tissue microarray sample analysis

Tissue microarrays (TMAs) for colon adenocarcinoma were purchased from US Biomax. IHC was performed using antibodies against REG4 (R&D Systems, Minneapolis, MN, AF1379; 1:200), p-ERK (T202/Y204; Cell Signaling Technology, Danvers, MA, 4370S; 1:1,000), anti-CD44 (Proteintech, 15675-1-AP; 1:100) or CD133 (Miltenyi, Bergisch Gladbach, Germany, 130-090-422; 1:100). The TMA slides were visualized by microscopy (Nikon TE-2000U). For quantitative analysis, H-Score of each staining was determined using the IHC profiler software. H-Score = 3 × highly positive population

+ 2 × Positive population + 1 × weakly positive population + 0 × negative population.

Tumor organoid culture

Fresh tumor tissue samples were processed as previously described,[30] with several modifications. The tissue was cut into small pieces, washed with ice-cold PBS thrice and subsequently digested with 0.25% trypsin (Invitrogen) at 37°C for 30 min. The single tumor cells filtered through a 40 μm cell strainer (Falcon) were centrifuged at 500*g* for 3 min at 4°C. The cell pellet was resuspended in Matrigel (growth factor reduced; Corning) and seeded into 48-well culture plates (500 cells/30 μl Matrigel). The tumor organoids were cultured in N2 medium as previously described.[31] The following niche factors were used: mouse recombinant Noggin (100 ng/ml; PeproTech) and 10% R-spondin-1 conditioned medium. To investigate the effect of REG4, which is induced by Ras/ERK pathway, 5 ng/ml mouse recombinant EGF was used. Medium was changed every 2 days.

Live-cell imaging

Coverslips were placed into six-well plates and tumor organoids were plated on the coverslips. The coverslips were then moved to the Chamlide TC chamber (Live Cell Instrument) and mounted onto a Nikon Ti-eclipse microscope (Nikon) equipped with a Chamlide TC incubator system (Live Cell Instrument), which maintains 37°C and 5% CO_2 humidity for live-cell imaging. The single organoids were imaged using a time-lapse video microscope. The videos of the organoids were constructed using NIS-Elements AR 3.1 (Nikon). Screenshots were captured from the movie file and represented as images at several time points.

Bioinformatics and statistics

Survival analyses were carried out using the Kaplan–Meier method with R2 web platform, which is publicly available at http://r2.amc.nl. Differences between survival distributions were analyzed using the log-rank test. Statistical computations were performed using GraphPad Prism6. LDA for frequency determinations as well as the corresponding *p* values were generated using the ELDA software, which took into account whether the assumptions for LDA were met (http://bioinf.wehi.edu.au/software/elda/index.html, provided by the Walter and Eliza Hall Institute).[29] Experimental data are presented as mean ± SD. Statistical significance was assessed by two-tailed unpaired Student's *t*-test.

See Supplementary Materials and Methods for plasmids, establishment of stable cell lines, CRISPR/Cas9 knockout system, flow cytometry analysis, REG4 enzyme-linked immunosorbent assay (ELISA), immunoblotting, immunohistochemistry, immunocytochemistry, X-gal staining, Reporter assay, quantitative real-time PCR (qRT-PCR), GSEA and quantification of signal intensity.

Data availability

Microarray data that support the findings of our study have been deposited in Gene Expression Omnibus (GEO) with the accession code "GSE119197".

Results

As reported previously,[16,17] both *APC* and *KRAS* mutations synergistically stabilize β-catenin and Ras resulting in strong activation of both Wnt/β-catenin and Ras/ERK signaling pathways, and can significantly induce the expression of CSCs markers in comparison with *APC* or *KRAS* mutation alone (Supporting Information Fig. S1A). On this basis, the crucial role of *KRAS* mutation was discovered in the enhancement of CSCs characteristics in CRC cells harboring *APC* mutation (Supporting Information Figs. S1B and S1C).[16]

To systematically identify mutant *KRAS*-induced factors involved in promoting CSCs in CRC cells that lack *APC*, we performed microarray analyses to examine differentially expressed genes between the adherent (AD) and SP cells derived from both D-WT and D-MT cells (Fig. 1*a*). Genes that showed differential expression of more than 1.5 times between D-WT and D-MT cells in the SP (Supporting Information Table S1) and AD (Supporting Information Table S2) groups were subjected to heatmap analysis. Within the SP group, genes known to be involved in promoting CSCs, such as *IL8*,[32] *PHLDA1*,[33] *S100A4*,[34] *CD133* (*PROM1*)[35] and *S100A6*,[34] showed higher expression in D-MT than in D-WT cells, and most of these genes also showed similar expression pattern in the AD group (Supporting Information Fig. S2A). The effect of mutated *KRAS* on expression of these references genes was greater in the SP group than in AD group, and almost all of them showed the highest expression level in SP D-MT cells (Fig. 1*b*, Supporting Information Fig. S2B and Table S3). Overall, SP cells reflect the induction of CSCs by mutant *KRAS* better than AD cells, and it can thus be inferred that the mediators enhancing CSCs characteristics are induced by mutant *KRAS* more in the SP cells than in AD cells. The top 10 genes that exhibited greater expression changes by mutant *KRAS* in SP groups than in AD groups, and also had the highest expression level in SP D-MT cells, were selected as candidates for mediating promotion of CSCs properties induced by mutant *KRAS* (Fig. 1c and Supporting Information Table S4). Promotion of CSCs by mutant *KRAS* in CRC cells harboring *APC* mutation occurs through initial activation of β-catenin signaling, which is subsequently enhanced by stabilized mutant KRAS *via* a positive feedback loop through the MEK–ERK pathway.[16] Therefore, the feasibility of the mutant *KRAS*-induced genes during promotion of CSCs properties was validated by demonstrating a reduction in the expression of these genes upon treatment with an MEK inhibitor (Supporting Information Fig. S2C). Taken together, our results show that the candidates affecting CSCs properties are specifically induced in the SP derived from the *APC*-mutated DLD-1 cells harboring MT-*KRAS*, but not WT-*KRAS*.

REG4 was identified as the most prominent mediator promotion of CSCs properties induced by mutant *KRAS*

To select the most effective mediator enhancement of CSCs characteristics among the candidate genes, we used a filtering

strategy (Fig. 1*h*). For most of the candidate genes, fold change values by *KRAS* mutation were more than 1.5 times higher in the SP cells than in AD cells (Figs. 1*d* and 1*j* and Supporting Information Fig. S2D). CRISPR/Cas9-mediated knockout analyses revealed that REG4-knockout showed the most severe reduction in both the number and size of SP (Figs. 1*e*–1g and Supporting Information Fig. S3A). Eventually, REG4 was identified as the most effective factor endowing SP-forming ability and selected for further analysis involved in enhancement of CSCs properties.

Since REG4 is a secreted molecule, the production pattern (bottom) as well as mRNA level (top) of REG4 were analyzed in the AD and SP cells derived from both D-WT and D-MT cells. Both the mRNA and secreted protein levels of REG4 were elevated in the culture medium of SP derived from D-MT cells (Fig. 1*i*). Also, REG4 expression patterns were

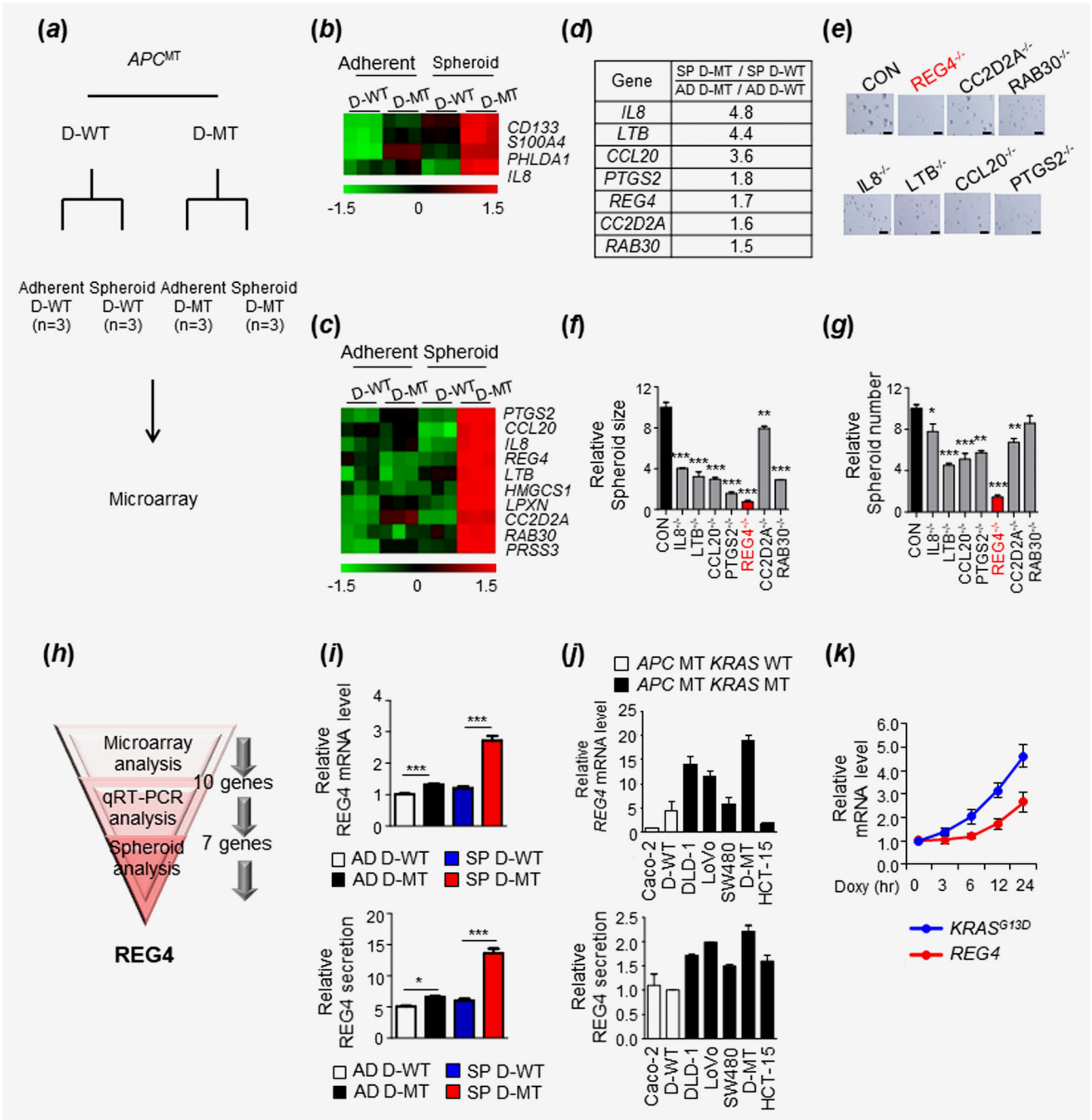

Figure 1. Legend on next page.

investigated in several different CRC cell lines with or without *KRAS* mutation in the presence of *APC* mutation. The mRNA level (Fig. 1*j*; top) and secreted (Fig. 1*j*; bottom) and endogenous (Supporting Information Fig. S3B) protein levels of REG4 were higher in all mutant *KRAS* cell lines than that in the wild-type *KRAS* cell lines. In addition, the mRNA expression level of *LGR5*, the CSCs marker, was higher in the mutant *KRAS* cell lines (Supporting Information Fig. S3C). Furthermore, the *REG4* induction was confirmed by doxycycline-induced $KRAS^{G13D}$ overexpression (Fig. 1*k*). Overall, these data suggest that REG4 is a factor that can affect CSCs properties induced by mutant *KRAS*.

REG4 regulates CSCs properties in CRC cells

A critical role of REG4 as a factor mediating promotion of CSCs characteristics was shown by both shRNA-mediated knockdown and CRISPR/Cas9-mediated knockout experiments, which demonstrated dosage-dependent reduction in SP-making capabilities (Fig. 2*a*). The role of REG4 in enhancement of CSCs properties was confirmed by reduction in expression of CSCs markers, including CD44, CD133 and CD166 in SP D-MT $REG4^{-/-}$ cells (Supporting Information Fig. S4A). Since SP formation was severely suppressed by REG4 knockout, knockout experiments were replaced by knockdown experiments for thoughtful functional analyses of REG4. The proportions of both $CD44^+/CD133^+$ double-positive cells and $CD44^+/CD133^+/CD166^+$ triple-positive cells as well as the protein and mRNA levels of CSCs markers were decreased by REG4 knockdown in SP D-MT (Figs. 2*b*–2*d* and Supporting Information Fig. S4B). Additionally, the effect of REG4 knockdown was also confirmed in LoVo cells harboring mutant *KRAS* (Supporting Information Figs. S4C and S4D).

In contrast, both the size and number of SP were significantly increased in a dose-dependent manner in SP D-WT expressing low levels of REG4 by treatment with recombinant human REG4 protein (rhREG4; Fig. 2*e*). The proportions of CSCs markers positive cells and the protein levels as well as mRNA levels were increased by treatment with rhREG4 (Figs. 2*f*–2*h*). It was also confirmed in Caco-2 cells harboring wild-type *KRAS* (Supporting Information Figs. S4E and S4F). Moreover, the size and number of SP acquired by treatment with rhREG4 were similar to those of the SP D-MT (Supporting Information Fig. S5A), and mRNA expression of *REG4* was decreased by KRAS-knockdown in SP D-MT (Supporting Information Fig. S5B). Moreover, the decrease in size and number of SP by REG4-knockdown was restored by treatment with rhREG4 (Supporting Information Fig. S5C). Therefore, REG4 is a determining factor for CSCs characteristics of CRC cells harboring *APC* mutation.

REG4 expression correlates with CSCs markers in the small intestinal tumors from $Apc^{min/+}/Kras^{G12D}LA2$ mice and in CRC patients harboring both *APC* and *KRAS* mutations

To investigate whether REG4 expression is induced by mutant *KRAS in vivo*, the levels of REG4 were observed in crypts of both $Apc^{min/+}$ and $Apc^{min/+}/Kras^{G12D}LA2$ transgenic mice using immunohistochemical (IHC) analyses. We observed that $REG4^+$ cells localized at crypts of $Apc^{min/+}/Kras^{G12D}LA2$ mice exhibited much stronger staining intensity for REG4 as well as the increment of numbers of $REG4^+$ cells (Supporting Information Fig. S6A), and these observations confirm the induction of REG4 by *KRAS* mutation in CRC cells with *APC* mutation *in vivo*. Moreover, REG4 levels were higher in the small intestinal tumors of $Apc^{min/+}/Kras^{G12D}LA2$ mice, and REG4 levels colocalized with CD44, CD133 and CD166 in tumors from both $Apc^{min/+}$ and $Apc^{min/+}/Kras^{G12D}LA2$ mice (Figs. 3*a* and 3*b*). In addition, the levels of REG4 were also higher in mouse xenograft tumors from SP D-MT, and the induced REG4 colocalized with CD44 in tumor specimens of SP D-MT (Fig. 3*c*).

To extend these findings toward clinical implication, CRC patients were divided into two groups (high, low) according

Figure 1. Identification and characterization of REG4, a mutant *KRAS*-induced factor that mediates promotion of CSCs properties. (*a*) A scheme for preparation of cells for microarray analysis to identify factors involved in promotion of CSCs properties induced by *KRAS* mutation in *APC*-mutated CRC cells. DLD-KRAS-WT (D-WT) and DLD-KRAS-MT (D-MT) cells were grown under both adherent and spheroid conditions for 72 hr. (*b* and *c*) Heatmap analysis of microarray data. Raw signal intensities of each gene from the microarray results were converted into row Z-score and analyzed by using MeV v4.0 software ($n = 3$, each groups). Expression patterns of reference genes in all four groups (Adherent and spheroid cells derived from both D-WT and D-MT cells; *b* and Table S3). Expression patterns of top 10 candidate genes in all four groups (*c* and Table S4). (*d*) Quantitative real-time PCR (qRT-PCR) validation of candidate genes differentially expressed in adherent (AD) and spheroid (SP) cells derived from both D-WT and D-MT cells. The fold change of the candidate genes induced by mutant *KRAS* in SP cells relative to AD cells are indicated. Fold change ›1.5; $p < 0.05$. (*e*–*g*) SP formation assay for CRISPR/Cas9-mediated gene knockout screens in SP derived from D-MT cells. SP derived from D-MT knocked-out for different genes were captured at day 5 (*e*). The size (*f*) and number (*g*) of SP derived from D-MT cells were measured and quantified ($n = 3$). Scale bars, 200 μm. (*h*) A schematic summary of the strategy used for the selection of the prominent mediators enhancement of CSCs characteristics induced by *KRAS* mutation. (*i*) qRT-PCR analysis of *REG4* from the AD and SP cells derived from both D-WT and D-MT cells (top panel; $n = 3$) and ELISA analysis of secreted REG4 from the culture supernatant of the AD and SP cells derived from both D-WT and D-MT cells (bottom panel; $n = 3$). (*j*) qRT-PCR analysis of *REG4* from SP cells derived from CRC cell lines harboring either wild-type or mutant *KRAS* with *APC* mutation (toppanel; $n = 3$) and ELISA analysis of secreted REG4 from the culture supernatant of SP cells derived from CRC cell lines harboring either wild type or mutant *KRAS* with *APC* mutation (bottom panel; $n = 3$). (*k*) qRT-PCR analysis of time course of changes in mRNA levels of *REG4* and $KRAS^{G13D}$ after doxycycline-induced $KRAS^{G13D}$ expression in SP derived from D-WT cells ($n = 3$). $^*p < 0.05$, $^{**}p < 0.01$, $^{***}p < 0.001$. All data are the mean ± SD. *p* values were determined using unpaired Student's *t*-test. [Color figure can be viewed at wileyonlinelibrary.com]

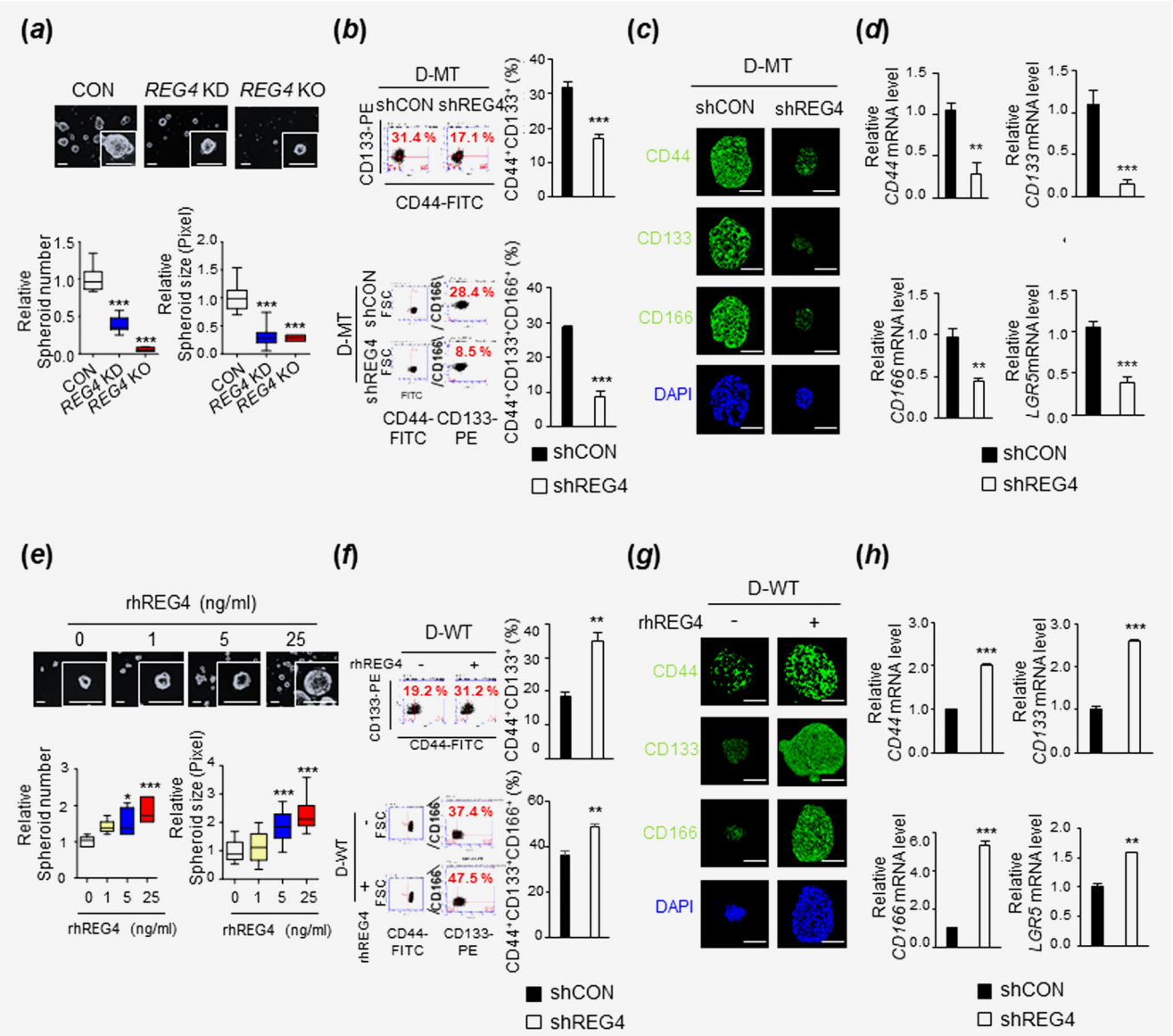

Figure 2. Effect of REG4 modulation on the formation of SP and induction of CSCs markers in D-MT and D-WT cells, respectively. (*a*) SP formation assay using D-MT cells with REG4 knocked down (KD) or knocked out (KO). The SP were captured at Day 5 (top panel), and the number (bottom left panel; $n = 3$) and size of SP were measured and quantified (bottom right panel; $n = 3$). Scale bars, 200 μm. (*b*) Flow cytometric analysis of the expression of CD44, CD133 and CD166 in SP derived from D-MT cells stably expressing a control shRNA (shCON) or shRNA targeting REG4 (shREG4). The proportion of $CD44^+/CD133^+$ double-positive cells (top panel) and $CD44^+/CD133^+/CD166^+$ triple-positive cells (bottom panel) was determined ($n = 3$). (*c* and *d*) Immunocytochemical (ICC) analysis (*c*) and qRT-PCR analysis (*d*) of CD44, CD133 and CD166 in SP derived from D-MT cells stably expressing shCON or shREG4 ($n = 3$). Scale bars, 50 μm. (*e*) SP formation assay using D-WT cells treated with or without rhREG4 for 5 days. SP were captured at Day 5 (top panel), and the number (bottom left panel; $n = 3$) and size of SP were measured and quantified (bottom right panel; $n = 3$). Scale bars, 200 μm. (*f*) Flow cytometric analysis of the expression of CD44, CD133 and CD166 in SP derived from D-WT cells treated with or without 25 ng/ml rhREG4. The proportions of $CD44^+/CD133^+$ double-positive cells (top panel) and $CD44^+/CD133^+/CD166^+$ triple-positive cells (bottom panel) were determined ($n = 3$). (*g* and *h*) ICC analysis (*g*) and qRT-PCR analysis (*h*) of CD44, CD133 and CD166 in SP derived from D-WT cells treated with or without 25 ng/ml rhREG4 ($n = 3$). Scale bars, 50 μm. $^*p < 0.05$, $^{**}p < 0.01$, $^{***}p < 0.001$. All data are the mean ± SD. *p* values were determined using unpaired Student's *t*-test. [Color figure can be viewed at wileyonlinelibrary.com]

to *REG4* mRNA expression levels. Interestingly, the prognosis of the patients expressing high *REG4* levels revealed a critically poor survival pattern (Fig. 3*d*). In addition, CRC patient cohort revealed that the expression level of *REG4* was significantly increased in patients with *KRAS* or *BRAF* mutations (Fig. 3*e*). The REG4 expression positively correlated with the

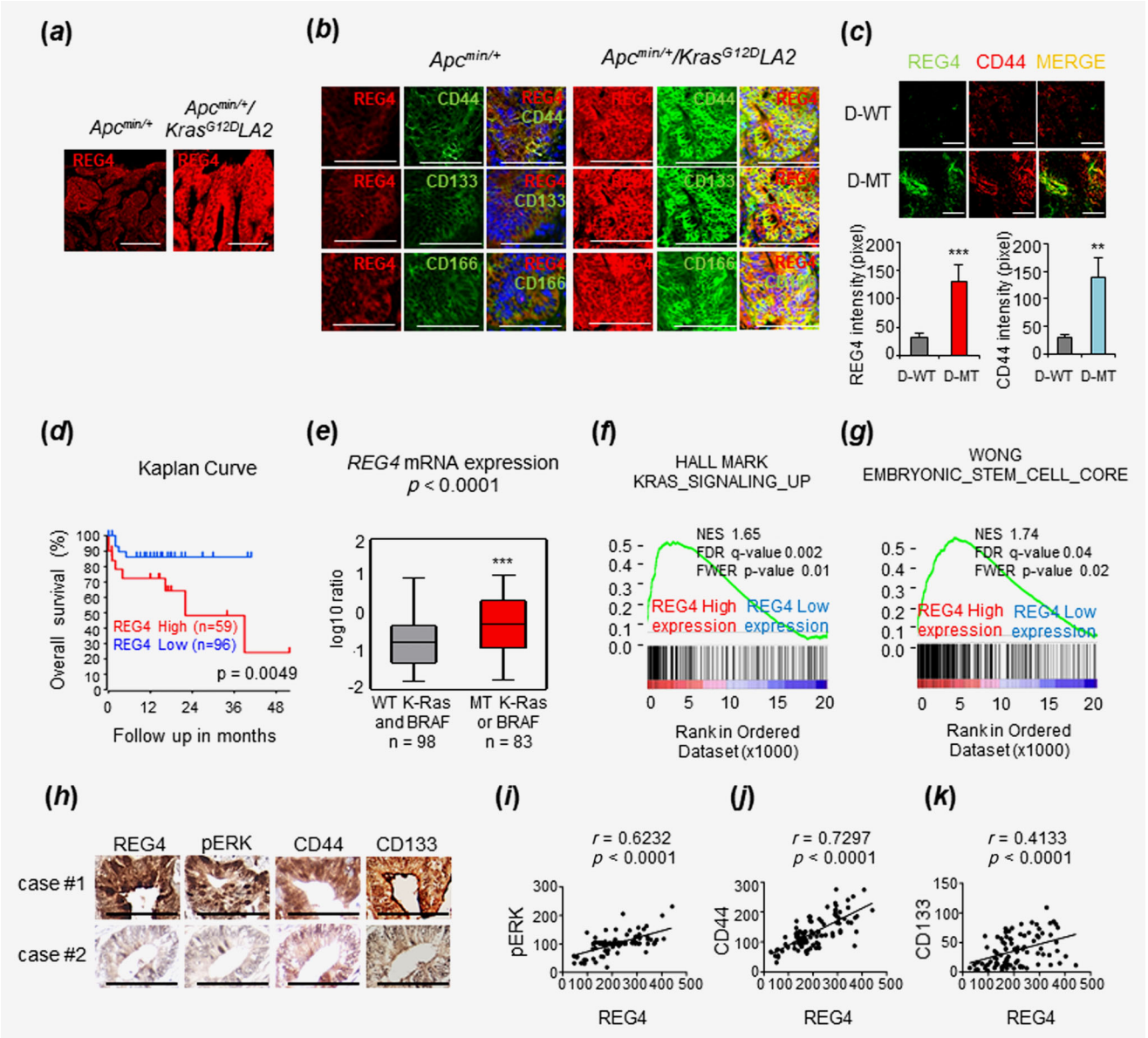

Figure 3. Expression profiles of REG4 and CSCs markers in the small intestinal tumors from $Apc^{min/+}/Kras^{G12D}LA2$ mice and in CRC patients where both *APC* and *KRAS* mutations are present. (*a* and *b*) Immunohistochemistical (IHC) analyses of small intestinal tumor from $Apc^{min/+}$ and $Apc^{min/+}/Kras^{G12D}LA2$ mice. Analysis of tissue sections incubated with the antibodies against REG4 (*a*) and CSCs markers (CD44, CD133 and CD166) (*b*). Scale bars, 100 μm. (*c*) IHC analysis of SP derived from both D-WT and D-MT cells injected subcutaneously into NOD/SCID mice. The representative images were captured (top panel) and the mean intensity of the staining for REG4 and CD44 were measured and quantified (bottom panel; $n = 3$). $^{**}p < 0.01$, $^{***}p < 0.001$. Scale bars, 100 μm. (*d*) Kaplan–Meier curves for overall survival of colon cancer patients classified by *REG4* expression using the R2 Genomics Analysis and Visualization Platform in a Mixed Colon Adenocarcinoma dataset. REG4 High › 5.840, $n = 59$; REG4 Low ‹ 5.840, $n = 96$. *p* values were obtained using the log-rank test (Mantel-Cox). (*e*) Box plot of *REG4* mRNA expression in colon cancer patient genotypes classified by wild-type (WT) *KRAS* and WT *BRAF* ($n = 98$), mutant (MT) *KRAS* or MT *BRAF* ($n = 83$; GEO: GSE42284). (*f* and *g*) Gene Set Enrichment Analysis (GSEA) plots of gene expression signatures in CRC patients (GEO: GSE13294) according to *REG4* mRNA expression levels; genes upregulated in the high expression of *REG4* are enriched in signatures of mutant *KRAS*-upregulating genes (HALL MARK KRAS_SIGNALING_UP) (*f*) and stemness-regulating genes (WONG EMBRYONIC_STEM_CELL_CORE) (*g*). The bar-code plot indicates the positions of genes in each gene set; red and blue colors represent positive and negative Pearson correlations with *REG4* expression, respectively. NES, normalized enrichment score; FDR, false discovery rate; FWER, family-wise-error rate. (*h–k*) IHC analyses for the indicated proteins from CRC tissue microarray (TMA). The representative images were presented (*h*) and correlation between the expression levels of REG4 and pERK (*i*), CD44 (*j*) and CD133 (*k*), respectively, on TMA ($n = 91$) were evaluated. Pearson R correlation analysis was performed. Scale bars, 200 μm. $^{**}p < 0.01$, $^{***}p < 0.001$. All data are the mean ± SD. *p* values were determined using unpaired Student's *t*-test. [Color figure can be viewed at wileyonlinelibrary.com]

expression of a hallmark gene set of mutant *KRAS*-upregulated genes[36] (Fig. 3*f*) as well as the *KRAS*-dependent gene expression signature[37] (Supporting Information Fig. S6B) in the CRC patient dataset. Moreover, a strong enrichment of genes linked to CSCs gene signature was observed in patients with high *REG4* expression (Fig. 3*g*[38] and Supporting Information Fig. S6C[39]). The link between mutant *KRAS*-induced REG4 expression and CSCs induction was further supported through a TMA analysis of 91 patients with colorectal adenocarcinoma. The expression of REG4 positively correlated with

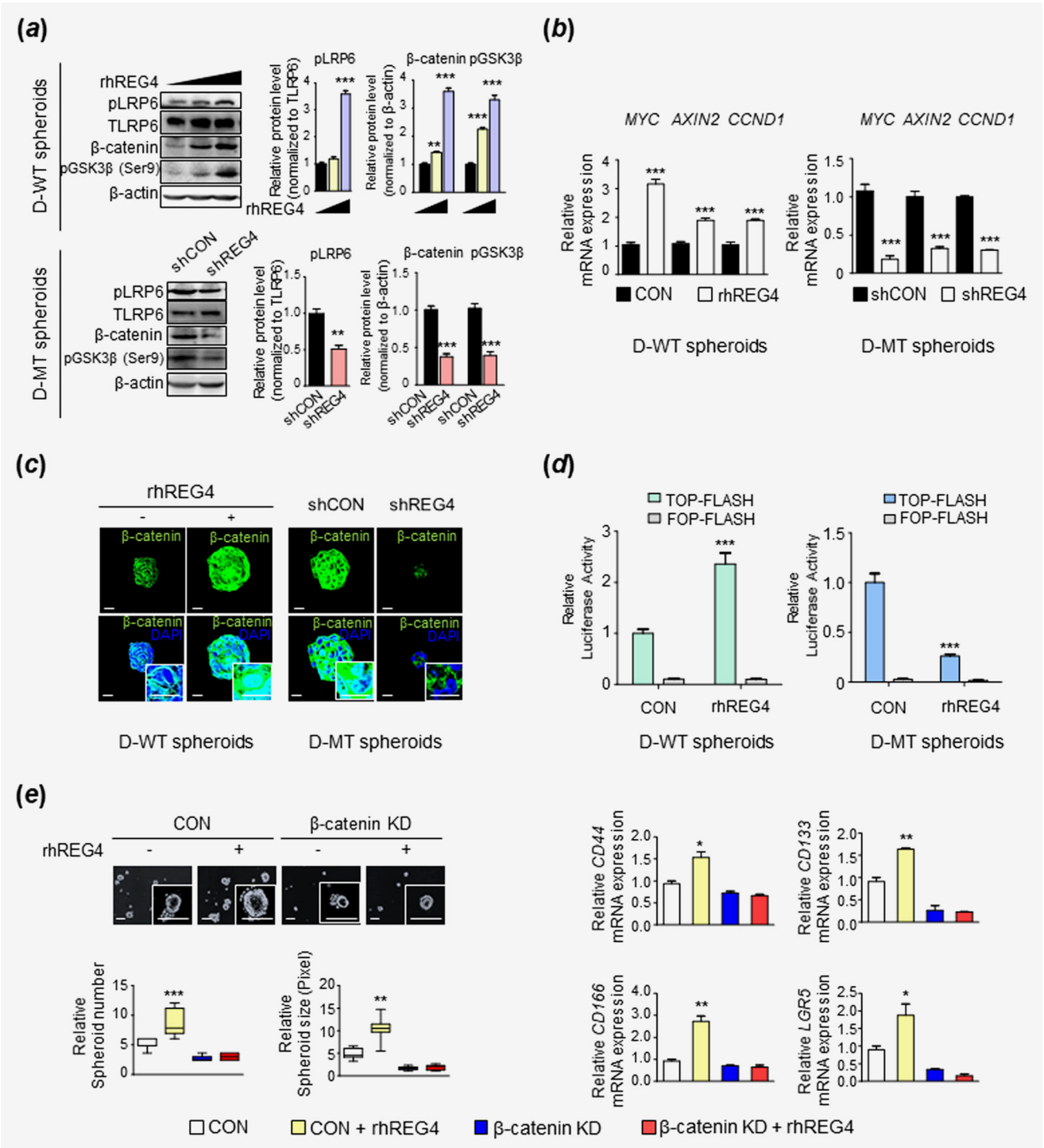

Figure 4. Legend on next page.

the expression of p-ERK, a downstream effector of Ras/ERK pathway, and also with the expressions of CD44 and CD133 (Figs. 3*h*–3*k*). These results from animal models and clinical studies corroborate that an increased expression of REG4 by *KRAS* mutation is closely associated with an enhanced expression of CSCs markers in CRC tissues.

REG4 promotes CSCs characteristics *via* the Wnt/β-catenin pathway

The Wnt/β-catenin pathway is considered as a critical route for the maintenance of stemness in CRC cells.[40,41] We tested the effects of REG4 on the activation of Wnt/β-catenin signaling in CRC cells with *APC* mutation. The protein levels of p-LRP6, β-catenin and p-GSK3β (Ser9) were increased in a dose-dependent manner in rhREG4-treated SP D-WT cells, whereas the levels were markedly decreased in SP REG4 knockdown D-MT cells (Fig. 4*a*) indicating that REG4 activates Wnt/β-catenin signaling at the level of receptor activation. To investigate the involvement of the Wnt receptors and co-receptors in REG4-mediated activation of Wnt/β-catenin signaling, we measured the effect of recombinant human DKK1 (rhDKK1), the LRP5/6 inhibitor, and also monitored the effect of REG4 by knockdown of the FZD receptors and LRP5/6 coreceptors (Supporting Information Figs. S7A and S7B). Treatment with rhDKK1 or knockdown of FZD receptors and LRP5/6 coreceptors reversed the changes resulted from the rhREG4 treatment. Therefore, these data suggest that FZD and LRP5/6, both upstream components of Wnt/β-catenin pathway, are involved in the REG4-mediated activation of Wnt/β-catenin pathway. Furthermore, the mRNA expression levels of downstream target genes of Wnt/β-catenin signaling were either increased by rhREG4 treatment or decreased by shREG4 introduction (Fig. 4*b*). Also, the nuclear accumulation of β-catenin and luciferase reporter activity were either increased by rhREG4 treatment or decreased by shREG4 introduction (Figs. 4*c* and 4*d*). Moreover, shRNA-mediated knockdown of β-catenin abolished the rhREG4-induced the promotion of CSCs properties (Fig. 4*e*), thereby indicating that REG4 enhances CSCs characteristics in a β-catenin-dependent manner.

REG4 enhances CSCs properties in tumor organoids

To further investigate the effect of REG4 on CSCs properties of tumor organoid, we treated organoids of the small intestinal tumor from *Apc*$^{min/+}$*/Lgr5-EGFP* mice with recombinant mouse REG4 (rmREG4). The growth of tumor organoids was significantly increased by rmREG4 treatment (Figs. 5*a* and 5*b*; Supporting Information Movies S1 and S2). The CSCs markers were enhanced in rmREG4-treated organoids than in control organoids, as shown by ICC (Fig. 5*c*) and qRT-PCR (Fig. 5*d*) analyses. Also, the protein levels of β-catenin (Figs. 5*c* and 5*e*), p-GSK3 beta (Ser9) and p-LRP6 were increased in rmREG4-treated organoids (Fig. 5*e*). Furthermore, the Axin2-LacZ reporter activity of the organoids from *Apc*$^{min/+}$*/Axin2*^{lacZ} mice was much higher in rmREG4-treated organoids (Fig. 5*f*). Overall, REG4 plays a critical role in promotion of CSCs characteristics in mouse-derived tumor organoids *via* activation of the Wnt/β-catenin signaling.

REG4 plays roles in the promotion of CSCs properties as well as initiation and growth of tumors in mouse xenograft model

To identify the role of REG4 in CRC tumorigenesis *in vivo*, we examined whether REG4 inhibition could block tumor growth of D-MT cells in a mouse xenograft model. We therefore subcutaneously implanted D-MT cells stably expressing a control shRNA or shRNA targeting *REG4* (shRNA #1 or #2) into nude mice. REG4-knockdown D-MT cells exhibited slower tumor growth and formed smaller size tumors (Supporting Information Fig. S8A). In addition, mRNA and protein levels of CSCs markers as well as Wnt target genes were reduced in REG4-knockdown tumors (Supporting Information Fig. S8B and S8C).

To further identify the role of REG4 involved in the tumor-initiating capacity and enhancement of CSCs characteristics *in vivo*, we performed LDA.[42–44] The tumor forming capability of the REG4-knockdown SP was notably lowered as shown by injection of different numbers of cells (Figs. 6*a* and 6*b*). REG4-knockdown led to more than 90% reduction in frequency of CSCs (Fig. 6*c*), indicating that tumor-initiating capacity and population of CSCs were significantly abolished

Figure 4. Effect of REG4 on Wnt/β-catenin signaling. (*a*) Immunoblot (IB) analysis of the effect of REG4 on SP derived from D-WT (top panel) and D-MT cells (bottom panel), respectively. SP cells derived from D-WT cells were treated with or without rhREG4 for 5 days in a dose-dependent manner (5, 25 ng/ml). SP cells derived from D-MT cells stably expressing shCON or shREG4 were cultured for 5 days. Whole cell lysates (WCLs) were prepared and probed with antibodies recognizing the indicated proteins. All blots show representative images ($n = 3$) and quantified. Western Blot bands are derived from separate experiments but only one representative loading control is shown. (*b*) qRT-PCR analysis of Wnt target genes (*MYC*, *AXIN2* and *CCND1*) in SP derived from D-WT cells treated with or without 25 ng/ml rhREG4 and SP derived from D-MT cells stably expressing shCON or shREG4, respectively ($n = 3$). (*c*) ICC analysis of β-catenin in SP derived from D-WT cells treated with or without 25 ng/ml rhREG4 and SP derived from D-MT cells stably expressing shCON or shREG4, respectively. Scale bars, 25 μm. (*d*) TOPflash luciferase reporter assays in SP derived from D-WT cells treated with or without 25 ng/ml rhREG4 and SP derived from D-MT cells stably expressing shCON or shREG4, respectively. FOPflash reporter was used as the negative control. (*e*) Effects of shRNA-mediated β-catenin knockdown on REG4-mediated promotion of CSCs properties. SP derived from β-catenin knockdown (KD) D-WT and control cells (CON) were treated with or without 25 ng/ml rhREG4 for 5 days. The SP were captured on Day 5 (top left panel), and the number and size of SP were measured and quantified (bottom left panel; $n = 3$). qRT-PCR analysis of CSCs markers (*CD44*, *CD133*, *CD166* and *LGR5*) were performed in indicated cells (right panel). Scale bars, 500 μm. $*p < 0.05$, $**p < 0.01$, $***p < 0.001$. All data are the mean ± SD. *p* values were determined using unpaired Student's t-test. [Color figure can be viewed at wileyonlinelibrary.com]

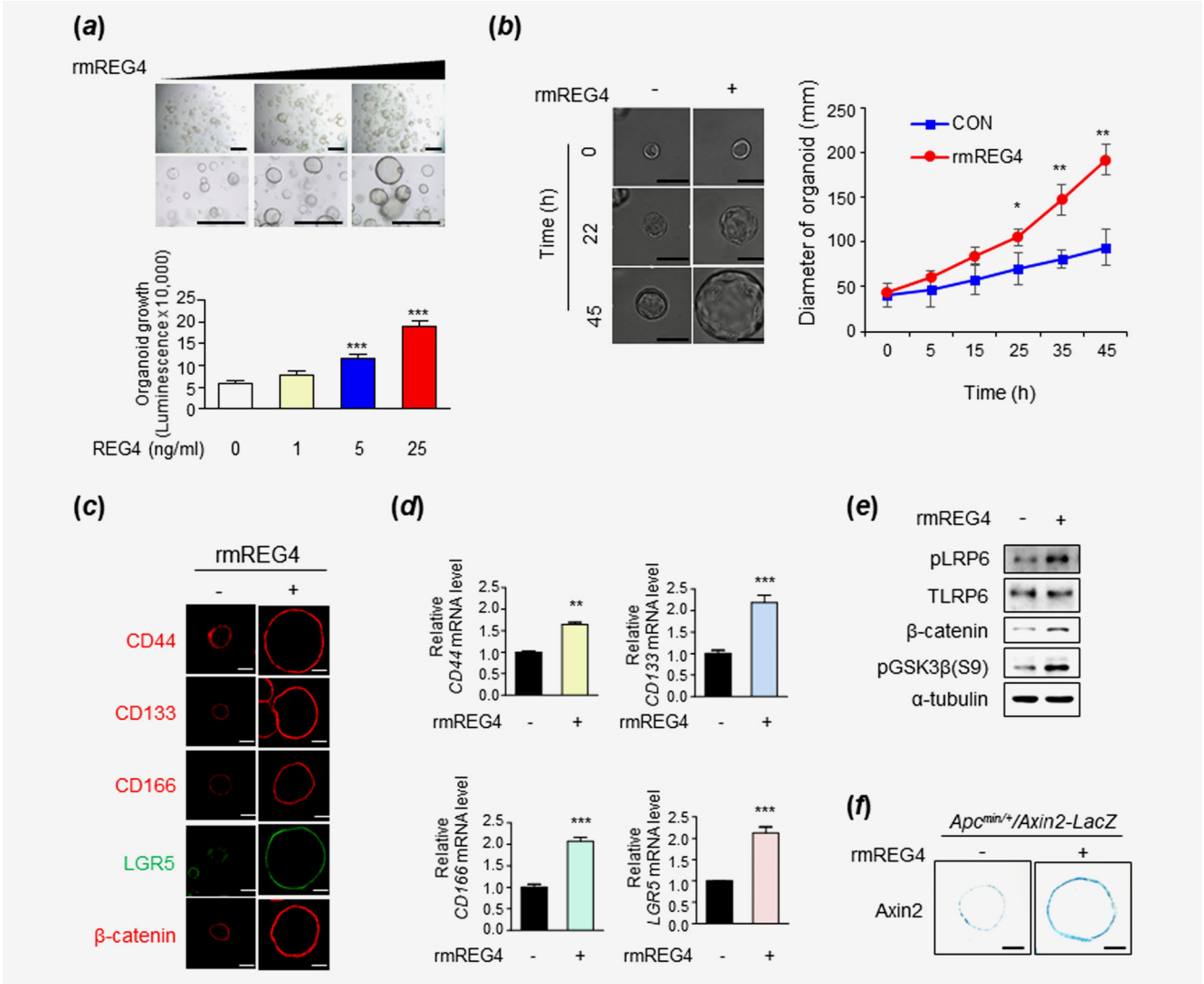

Figure 5. Effect of REG4 modulation on CSCs properties in tumor organoids. (*a–e*) Effect of recombinant mouse REG4 (rmREG4) treatment on organoids of small intestinal tumor from *Apc*$^{min/+}$*/Lgr5-EGFP* mice. The tumor organoids were treated with or without rmREG4 for 7 days in a dose-dependent manner (*a*). The tumor organoids were captured at Day 7 (top panel), and the growth of organoids was measured using CellTiter-Glo cell viability assay (bottom panel; $n = 3$). ***$p < 0.001$. Scale bars, 500 μm. The tumor organoids were treated with or without 25 ng/ml rmREG4 for 45 hr (*b*). Time-lapse image of tumor organoids captured at the indicated times (0, 22, and 45 hr). Scale bars, 50 μm. ICC analysis of CD44, CD133, CD166, LGR5 and β-catenin (*c*) and qRT-PCR analysis of CD44, CD133, CD166 and LGR5 (*d*) in organoids treated with or without 25 ng/ml rmREG4 for 5 days. Scale bars, 50 μm. IB analysis of tumor organoids treated with or without 25ng/ml rmREG4 for 5 days (*e*). WCLs were prepared and probed with antibodies against the indicated proteins. All blots show representative images ($n = 3$). Western Blot bands are derived from separate experiments but only one representative loading control is shown. (*f*) β-Galactosidase staining of the organoids of small intestinal tumor from *Apc*$^{min/+}$*/Axin2*^{lacZ} mice. The tumor organoids were treated with or without 25ng/ml rmREG4 for 7 days. Scale bars, 100 μm. *$p < 0.05$, **$p < 0.01$, ***$p < 0.001$. All data are the mean ± SD. *p* values were determined using unpaired Student's *t*-test. [Color figure can be viewed at wileyonlinelibrary.com]

by REG4-knockdown. Furthermore, both tumor growth and tumor mass were suppressed in all REG4-knockdown groups (Figs. 6*d* and 6*e*). The levels of CSCs markers as well as Wnt/β-catenin signaling target genes were reduced in REG4-knockdown tumors, as shown by IHC (Fig. 6*f*) and qRT-PCR analyses (Fig. 6*g*). The protein levels of β-catenin (Figs. 6*f* and 6*h*), p-GSK3 beta (Ser9) and p-LRP6 were also significantly reduced by REG4-knockdown (Fig. 6*h*). Overall, REG4-knockdown severely abolishes tumorigenicity and characteristics of CSCs as well as tumor growth *in vivo via* the Wnt/β-catenin signaling pathway.

Discussion

Both *APC* and *KRAS* mutations synergistically activate CRC tumorigenesis involved in enhancement of CSCs characteristics. *KRAS* mutation plays a crucial role in the promotion of CSCs properties in CRC, and which occurs in *APC*-mutated CRC cells.[16] The CSCs induction by both *APC* and *KRAS* mutations

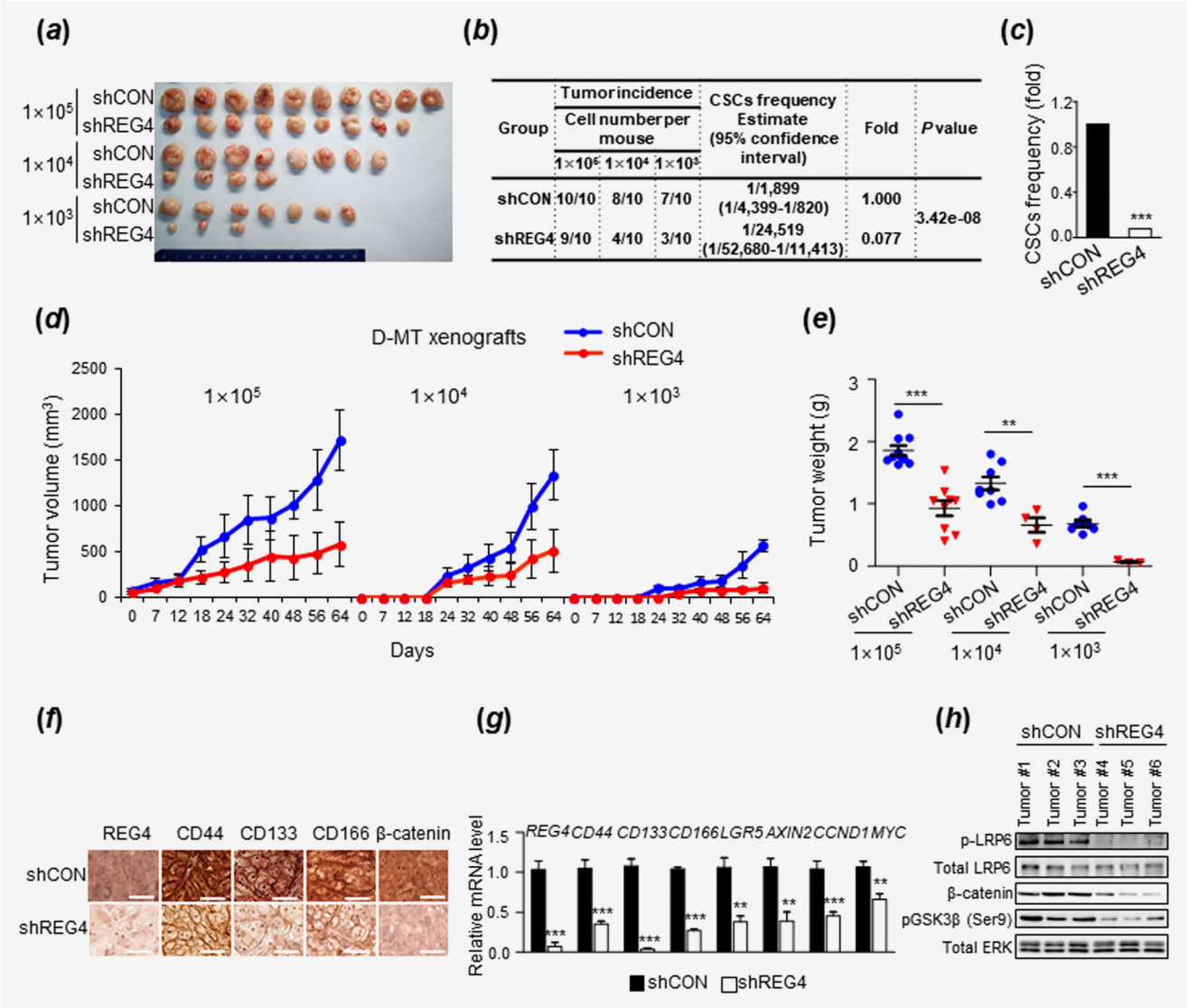

Figure 6. Effect of REG4 knockdown on the tumor-initiating capacity and CSCs properties in a mouse xenograft model. (*a–h*) *In vivo* limiting dilution analysis (LDA) was performed to assess the tumor-initiating capacity induced by REG4. Three doses (1×10^5, 1×10^4 and 1×10^3 cells) of SP derived from D-MT cells stably expressing shCON or shREG4 were subcutaneously injected into NOD/SCID-IL2Rγ$^{-/-}$ (NSG) mice. Representative images show respective xenograft tumors at Day 74 post subcutaneous injection (*a*). Frequency of CSCs in SP derived from D-MT cells stably expressing shCON or shREG4 as shown by the detailed data in tables (*b*), and a plot of fold change (*c*). Frequency estimates were computed using the ELDA software. Tumor volumes of mice were measured every 6–8 days (*d*) and tumor weight was measured at the time of sacrifice (*e*). Data represent mean ± SD (10 mice per group). IHC analysis for the indicated proteins from tumors of SP derived from D-MT cells stably expressing shCON or shREG4 (*f*; xenografted with 1×10^4 cells per mouse). Scale bars, 50 μm. qRT-PCR analysis of *REG4*, CSCs markers (*CD44*, *CD133*, *CD166* and *LGR5*) and Wnt/β-catenin signaling target genes (*AXIN2*, *CCND1* and *MYC*) in tumors of SP derived from D-MT cells stably expressing shCON or shREG4 (*g*; xenografted with 1×10^4 cells per mouse) ($n = 3$). IB analysis of xenografted tumor tissue with 1×10^4 cells per mouse (*h*). WCLs were prepared and probed with antibodies against the indicated proteins. All blots show representative images ($n = 3$). Western Blot bands are derived from separate experiments but only one representative loading control is shown. In (*b*, *c*), significance was measured by Pearson's Chi-squared test using ELDA software. In (*e*, *g*), $^{**}p < 0.01$, $^{***}p < 0.001$. All data are the mean ± SD. [Color figure can be viewed at wileyonlinelibrary.com]

is attributed to the hyperactivation of β-catenin signaling by its initial activation by *APC* loss and subsequent strong activation by stabilization of mutant KRAS protein generating the positive feedback loop through the MEK–ERK pathway.[10,16]

In our study, by using microarray-based transcriptional analysis, genes induced by *KRAS* mutation were systematically and convincingly investigated using *APC*-mutated D-WT and D-MT cells harboring wild-type and mutant *KRAS*, respectively. This

global approach to identify genes involved in the promotion of CSCs properties by *KRAS* mutation was validated by the identification of genes already known to be related to the promotion of CSCs, such as *IL8*, *PHLDA1*, *S100A4*, *S100A6* and *PROM1*, in SP D-MT harboring *KRAS* mutation. The knockout of all the representative *KRAS*-inducible genes, including IL8, LTB, CCL20, TPGS2, REG4, CC2D2A and RAB30, resulted in reduction of both size and number of SP derived from D-MT. However, REG4-knockout showed the most significant reduction in SP-forming capability of the cells. Therefore, we characterized its role in the promotion of CSCs characteristics induced by *KRAS* mutations.

The REG4 expression is markedly upregulated in a mutant *KRAS*-dependent manner in both CRC cells and CRC patient tissues harboring *APC* mutation. The REG4 induction by *KRAS* mutation in CRC cells lacking *APC* is acquired *via* the RAS downstream ERK. This was shown by abolishment of the REG4 as well as other CSCs markers induced by mutant *KRAS* in *APC*-mutated CRC cells by treatment with a MEK inhibitor.[16] These results are consistent with gene expression profiles of rectal cancers patients showing that REG4 expression was increased in mutant *KRAS* tumor.[45] REG4 positively regulates CSCs markers in SP derived from CRC cells and in mice xenograft model system. We found that LGR5 was also induced by REG4, which agrees with the recent finding that $REG4^+$ deep crypt secretory cells promote organoid formation of single $LGR5^+$ colon stem cells.[26]

Promotion of CSCs is thought to be the critical cause of tumor malignancies leading to lethality of the patients.[14] Therefore, elucidation of the key molecular mechanisms of CSCs and identification of therapeutic targets is the current important issue of cancer research.[46,47] The *APC* and *KRAS* mutations occur at the initiation and progression of CRC, respectively[3–5]; however, mutations in both *APC* and *KRAS* critically increased both initiation and growth of tumors, and synergistically increased tumorigenesis, including liver metastasis, of xenograft CRC tumor cells accompanied with enhanced induction of CSCs.[16] These findings have provided an important clue regarding the molecular mechanism and regulatory pathways leading to promotion of CSCs.

In our study, clinical implications of a link between mutant *KRAS*-induced REG4 and promotion of CSCs characteristics is demonstrated by the positive correlation between them in dataset derived from a cohort of 155 CRC patients and tissue microarray analyses of 91 CRC patients. Furthermore, the pathological significance of REG4 in human CRC patient lethality is indicated by the poor prognosis of patients expressing high levels of REG4.

Overall, we identified a key factor, REG4, which mediates the promotion of CSCs properties induced by *KRAS* mutation in CRC with *APC* loss. The approach targeting REG4 could be a new strategy for development of anticancer drugs for CRC involved in CSCs.

Acknowledgements

We thank Dr. B. Vogelstein and K.W. Kinzler for providing the DLD-1 isogenic cells. We also thank Dr. Y.-Y. Kong for providing the B6.129P2-*Lgr5*$^{tm1(cre/ERT2)Cle}$/*J* (*Lgr5-EGFP*) mice. This work was supported by the National Research Foundation of Korea (NRF) grant funded by the Korean Government (MSIP) (grants 2016R1A5A1004694 and 2015R1A2A05001873; to K.Y. Choi). J.H. Hwang was supported by a Brain Korea 21 (BK21) Plus studentship from the NRF. This research was partially supported by the Graduate School of YONSEI University Research Scholarship Grants.

References

1. Fearon ER, Vogelstein B. A genetic model for colorectal tumorigenesis. *Cell* 1990;61:759–67.
2. Phelps RA, Chidester S, Dehghanizadeh S, et al. A two-step model for colon adenoma initiation and progression caused by APC loss. *Cell* 2009;137:623–34.
3. Kinzler KW, Vogelstein B. Lessons from hereditary colorectal cancer. *Cell* 1996;87:159–70.
4. Bos JL, Fearon ER, Hamilton SR, et al. Prevalence of ras gene mutations in human colorectal cancers. *Nature* 1987;327:293–7.
5. Brink M, de Goeij AF, Weijenberg MP, et al. K-ras oncogene mutations in sporadic colorectal cancer in The Netherlands cohort study. *Carcinogenesis* 2003;24:703–10.
6. Janssen KP, Alberici P, Fsihi H, et al. APC and oncogenic KRAS are synergistic in enhancing Wnt signaling in intestinal tumor formation and progression. *Gastroenterology* 2006;131:1096–109.
7. D'Abaco GM, Whitehead RH, Burgess AW. Synergy between Apc min and an activated ras mutation is sufficient to induce colon carcinomas. *Mol Cell Biol* 1996;16:884–91.
8. Harada N, Oshima H, Katoh M, et al. Hepatocarcinogenesis in mice with beta-catenin and ha-ras gene mutations. *Cancer Res* 2004;64:48–54.
9. Sansom OJ, Meniel V, Wilkins JA, et al. Loss of Apc allows phenotypic manifestation of the transforming properties of an endogenous K-ras oncogene in vivo. *Proc Natl Acad Sci U S A* 2006;103:14122–7.
10. Lee SK, Hwang JH, Choi KY. Interaction of the Wnt/beta-catenin and RAS-ERK pathways involving co-stabilization of both beta-catenin and RAS plays important roles in the colorectal tumorigenesis. *Adv Biol Regul* 2018;68:46–54.
11. Jeong WJ, Ro EJ, Choi KY. Interaction between Wnt/beta-catenin and RAS-ERK pathways and an anti-cancer strategy via degradations of beta-catenin and RAS by targeting the Wnt/beta-catenin pathway. *NPJ Precis Oncol* 2018;2:5.
12. Chaffer CL, Weinberg RA. A perspective on cancer cell metastasis. *Science* 2011;331:1559–64.
13. Schepers AG, Snippert HJ, Stange DE, et al. Lineage tracing reveals Lgr5+ stem cell activity in mouse intestinal adenomas. *Science* 2012;337:730–5.
14. Baccelli I, Trumpp A. The evolving concept of cancer and metastasis stem cells. *J Cell Biol* 2012; 198:281–93.
15. Feng Y, Bommer GT, Zhao J, et al. Mutant KRAS promotes hyperplasia and alters differentiation in the colon epithelium but does not expand the presumptive stem cell pool. *Gastroenterology* 2011;141:1003–13.
16. Moon BS, Jeong WJ, Park J, et al. Role of oncogenic K-Ras in cancer stem cell activation by aberrant Wnt/beta-catenin signaling. *J Natl Cancer Inst* 2014;106:djt373.
17. Jeong WJ, Yoon J, Park JC, et al. Ras stabilization through aberrant activation of Wnt/beta-catenin signaling promotes intestinal tumorigenesis. *Sci Signal* 2012;5:ra30.
18. Vanderlaag K, Wang W, Fayadat-Dilman L, et al. Regenerating islet-derived family member, 4 modulates multiple receptor tyrosine kinases and mediators of drug resistance in cancer. *Int J Cancer* 2012;130:1251–63.
19. Kuniyasu H, Oue N, Sasahira T, et al. Reg IV enhances peritoneal metastasis in gastric carcinomas. *Cell Prolif* 2009;42:110–21.
20. Rafa L, Dessein AF, Devisme L, et al. REG4 acts as a mitogenic, motility and pro-invasive factor for colon cancer cells. *Int J Oncol* 2010;36:689–98.
21. Kawasaki Y, Matsumura K, Miyamoto M, et al. REG4 is a transcriptional target of GATA6 and is essential for colorectal tumorigenesis. *Sci Rep* 2015;5:14291.

22. Bishnupuri KS, Luo Q, Murmu N, et al. Reg IV activates the epidermal growth factor receptor/Akt/AP-1 signaling pathway in colon adenocarcinomas. *Gastroenterology* 2006;130:137–49.
23. Bishnupuri KS, Sainathan SK, Bishnupuri K, et al. Reg4-induced mitogenesis involves Akt-GSK3beta-beta-catenin-TCF-4 signaling in human colorectal cancer. *Mol Carcinog* 2014;53(Suppl 1):E169–80.
24. Zhu X, Han Y, Yuan C, et al. Overexpression of Reg4, alone or combined with MMP-7 overexpression, is predictive of poor prognosis in colorectal cancer. *Oncol Rep* 2015;33:320–8.
25. Kaprio T, Hagstrom J, Mustonen H, et al. REG4 independently predicts better prognosis in non-mucinous colorectal cancer. *PLoS One* 2014;9:e109600.
26. Sasaki N, Sachs N, Wiebrands K, et al. Reg4+ deep crypt secretory cells function as epithelial niche for Lgr5+ stem cells in colon. *Proc Natl Acad Sci U S A* 2016;113:E5399–407.
27. Yun J, Rago C, Cheong I, et al. Glucose deprivation contributes to the development of KRAS pathway mutations in tumor cells. *Science* 2009;325:1555–9.
28. Sanjana NE, Shalem O, Zhang F. Improved vectors and genome-wide libraries for CRISPR screening. *Nat Methods* 2014;11:783–4.
29. Hu Y, Smyth GK. ELDA: extreme limiting dilution analysis for comparing depleted and enriched populations in stem cell and other assays. *J Immunol Methods* 2009;347:70–8.
30. Sato T, Stange DE, Ferrante M, et al. Long-term expansion of epithelial organoids from human colon, adenoma, adenocarcinoma, and Barrett's epithelium. *Gastroenterology* 2011;141:1762–72.
31. Sato T, Vries RG, Snippert HJ, et al. Single Lgr5 stem cells build crypt-villus structures in vitro without a mesenchymal niche. *Nature* 2009;459:262–5.
32. Hwang WL, Yang MH, Tsai ML, et al. SNAIL regulates interleukin-8 expression, stem cell-like activity, and tumorigenicity of human colorectal carcinoma cells. *Gastroenterology* 2011;141:279–91.
33. Sakthianandeswaren A, Christie M, D'Andreti C, et al. PHLDA1 expression marks the putative epithelial stem cells and contributes to intestinal tumorigenesis. *Cancer Res* 2011;71:3709–19.
34. Harris MA, Yang H, Low BE, et al. Cancer stem cells are enriched in the side population cells in a mouse model of glioma. *Cancer Res* 2008;68:10051–9.
35. Wu Y, Wu PY. CD133 as a marker for cancer stem cells: progresses and concerns. *Stem Cells Dev* 2009;18:1127–34.
36. Liberzon A, Birger C, Thorvaldsdottir H, et al. The molecular signatures database (MSigDB) hallmark gene set collection. *Cell Syst* 2015;1:417–25.
37. Singh A, Greninger P, Rhodes D, et al. A gene expression signature associated with "K-Ras addiction" reveals regulators of EMT and tumor cell survival. *Cancer Cell* 2009;15:489–500.
38. Wong DJ, Liu H, Ridky TW, et al. Module map of stem cell genes guides creation of epithelial cancer stem cells. *Cell Stem Cell* 2008;2:333–44.
39. Bhattacharya B, Miura T, Brandenberger R, et al. Gene expression in human embryonic stem cell lines: unique molecular signature. *Blood* 2004;103:2956–64.
40. Vermeulen L, De Sousa EMF, van der Heijden M, et al. Wnt activity defines colon cancer stem cells and is regulated by the microenvironment. *Nat Cell Biol* 2010;12:468–76.
41. de Sousa EM, Vermeulen L, Richel D, et al. Targeting Wnt signaling in colon cancer stem cells. *Clin Cancer Res* 2011;17:647–53.
42. O'Brien CA, Kreso A, Jamieson CH. Cancer stem cells and self-renewal. *Clin Cancer Res* 2010;16:3113–20.
43. Fang L, Cai J, Chen B, et al. Aberrantly expressed miR-582-3p maintains lung cancer stem cell-like traits by activating Wnt/beta-catenin signalling. *Nat Commun* 2015;6:8640.
44. Zhu P, Wang Y, Du Y, et al. C8orf4 negatively regulates self-renewal of liver cancer stem cells via suppression of NOTCH2 signalling. *Nat Commun* 2015;6:7122.
45. Garcia-Aguilar J, Chen Z, Warden C, et al. Gene expression profiles of rectal cancers with mutant or wild-type Kras. *J Clin Oncol* 2013;31:414.
46. Chen K, Huang YH, Chen JL. Understanding and targeting cancer stem cells: therapeutic implications and challenges. *Acta Pharmacol Sin* 2013;34:732–40.
47. Dragu DL, Necula LG, Bleotu C, et al. Therapies targeting cancer stem cells: current trends and future challenges. *World J Stem Cells* 2015;7:1185–201.